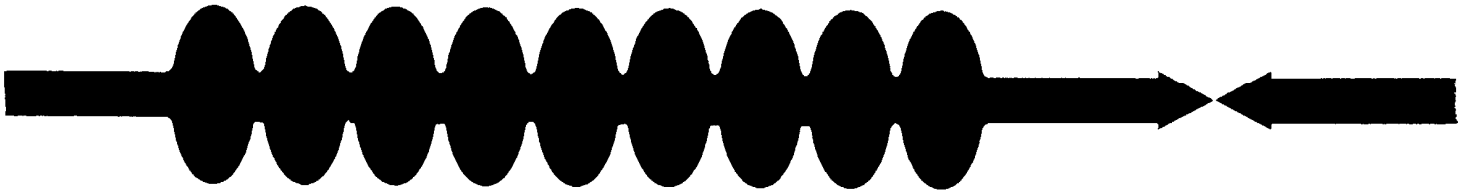

TESLA - COLLABORATION

Some Error Estimations for Beam Position Monitors

T. Scholz

TU Berlin

January 2000, TESLA 2000-01

SOME ERROR ESTIMATIONS FOR BEAM POSITION MONITORS

Thomas Scholz,
Technical University Berlin, EN-2, Einsteinufer 17, D10587, Germany

10.2.1999

1 Introduction

For high precision beam position monitors (BPM) a remarkable signal resolution is required. This means the measurements of very small signals. These small signals are sensitive to any kinds of errors. Beside the limits of the detection electronic errors can occur already at the origin of the signal due to geometrical errors. Manufacturing the beam pipe with the detection holes for the BPM involves some mechanical tolerances. Some of these will be treated here using two methods, the momentum method and Bethe hole coupling. The first one is very well suited to estimate the influence of beam tube shape variations. The second one gives an idea of allowed changes of the coupling hole or slot area as well as the shape of the slot.

2 Deviations at the Beam Tube

In this part the momentum method is applied to some variations in the shape of the beam tube. This momentum method is based on substituting metallic surfaces with ideal conductivity by equivalent replacement charges. For the determination of the value for each of these charges an integral equation has to be solved. In a numerical treatment, which means a finite number of charges, this leads to a system of linear equations. Additonally exciting elements, which can be real charges as well as current, are supposed to be placed everywhere.

Here the integral equation is solved for the Poisson equation. It is an adequate approximation even for this time dependent waveguide problem, because of the TEM-field of the beam, which corresponds with the electrostatic field of a line charge. Higher order modes are negligible because the working frequencies of the BPM's are assumed very below cutoff in the beam tube.

Furthermore the calculation is restricted to two dimensions. It fastens the computation strongly and on the other hand it covers most of the occuring aspects. Thus the exciting beam is represented by a line charge perpendicular to the calculation plane.
The beam tube radius in the following is 6 mm, which is the value for the undulator section in the TESLA-FEL.

2.1 An Excentric Beam in a Round Tube

This effect is mentioned to get an idea how big is the effect in terms of the static field strength for eccentered line charge representing the beam. So in figure 2.1 the relative difference of field strength for opposite scanning points in the direction of the beam shift is depicted versus the magnitude of the beam shift with two different scales. Linearity of the curve is lost beyond about $150\mu m$ beam shift.

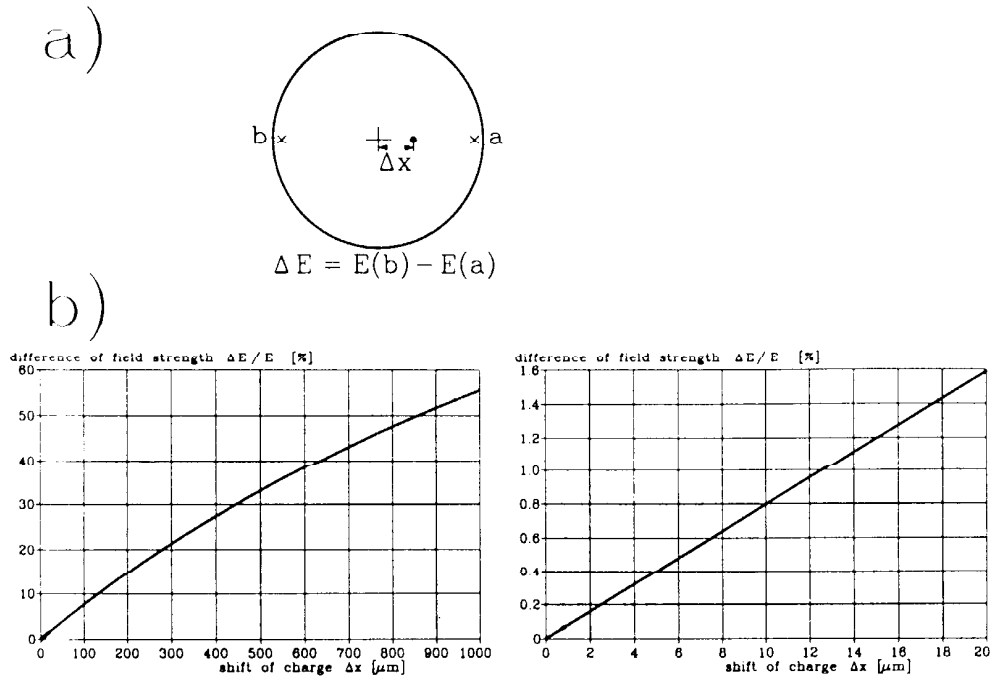

Figure 2.1: a) an eccentric beam in a round beam tube;
b) the difference of the BPM-signals versus the eccentricity of the beam.

2.2 Ellipticity of the Beam Tube

2.2.1 Ellipticity with a Centered Beam

The difference of the BPM-signals on the main axes, which means separated by an angle of 90°, is plotted versus the ellipticity in figure 2.2, expressed here as the difference of the length of the two main axes. The field strengths are taken at a constant distance from the beam tube wall. This relation is important for the estimation of getting different signals for the same beam shift in the two BPM-channels, which are separated by 90°, due to this kind of mechanical inaccuracy.

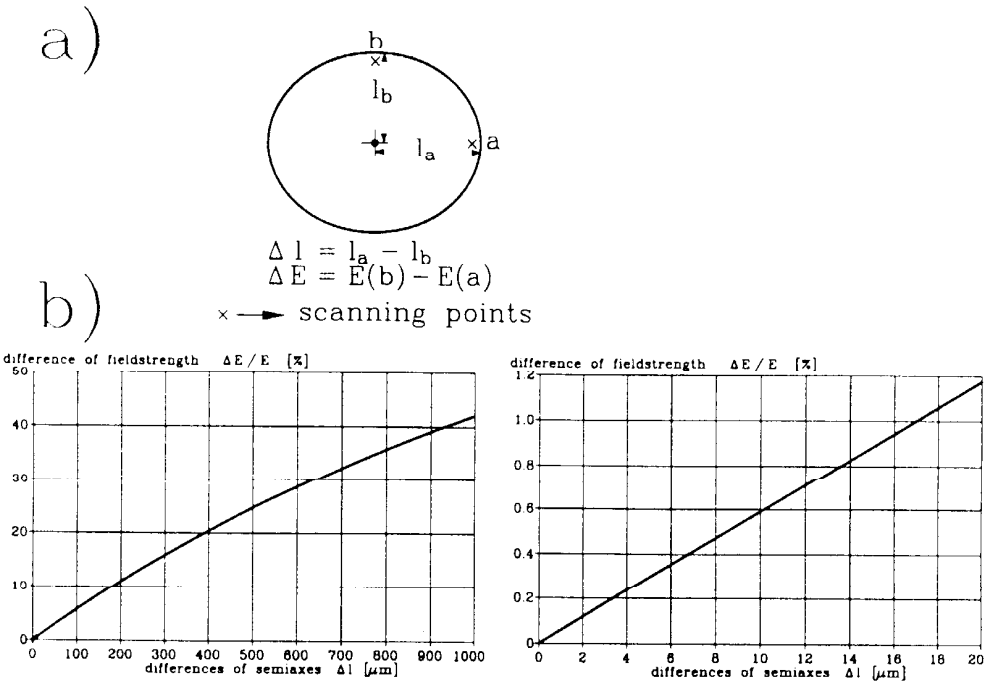

Figure 2.2: a) a centered beam in an elliptic beam tube;
b) the difference of the BPM-signals from the two main axes versus the length difference of the two main axes of the beam tube Δl taken at constant distance from the wall of the beam tube.

2.2.2 Influence of the Wall Thickness

For this investigation a TE_{01} wave mode is assumed for propagation in the wall slot. This is because the TEM-field couples through a slot parallel to the beam direction. For this mode the propagation constant below cutoff is calculated according to the formula

$$\beta_z = -j\beta_0\sqrt{\left(\frac{\nu_c}{\nu}\right)^2 - 1}$$

with $\beta_0 = 2\pi\nu/c_0$ and the cutoff frequency ν_c. The amplitude is taken from

$$A = \exp(-j\beta_z l)$$

with the wall thickness l.
The influence of deviations in the wall thickness of the beam tube in which the monitor slots are milled is shown in figure 2.3 for some slot widths and in figure 2.3a with a higher thickness resolution. The amplitude shift is referred to the maximum wall thickness of 2 mm. Walls with other thicknesses produce the same variation for the same thickness deviation.

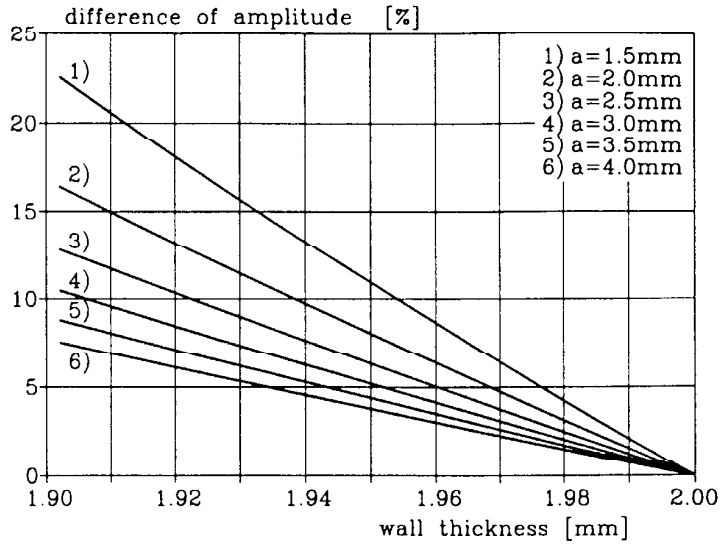

Figure 2.3: Change of wave amplitude in percentage versus the wall thickness for some slot widths a.

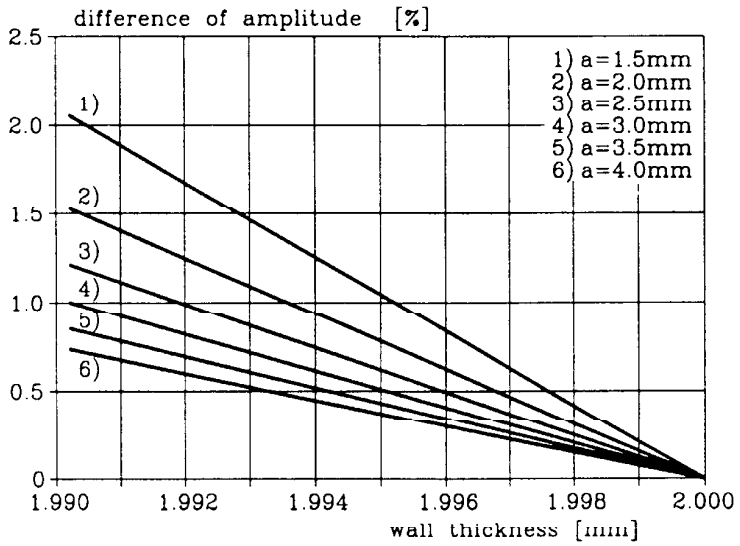

Figure 2.3a: Change of wave amplitude in percentage versus the wall thickness for some slot widths a.

2.2.3 Beam Shift Arbitrary to the Axes of the Ellipse

The location of the main axes of the elliptical deviation related to the beam shift will be statistical. So it is important to now the relative error versus the angle between the main axes and the direction of the beam shift.
In figure 2.4 the field strength along the wall of the beam tube is depicted versus the circumference angle counted from the great main axis onwards. $\Delta\varphi$ is thereby the angle between the main axis of the ellipse and the vertical offset of the beam.
If one turns to figure 2.5, where the difference of signals 180^o distant taken from figure 2.4 related to the signal difference of a circle are plotted for some ellipticities, it can be noticed, that these differences are much smaller than the differences between the maxima and minima in figure 2.4. This means that the arising error will barely exceed 3%.

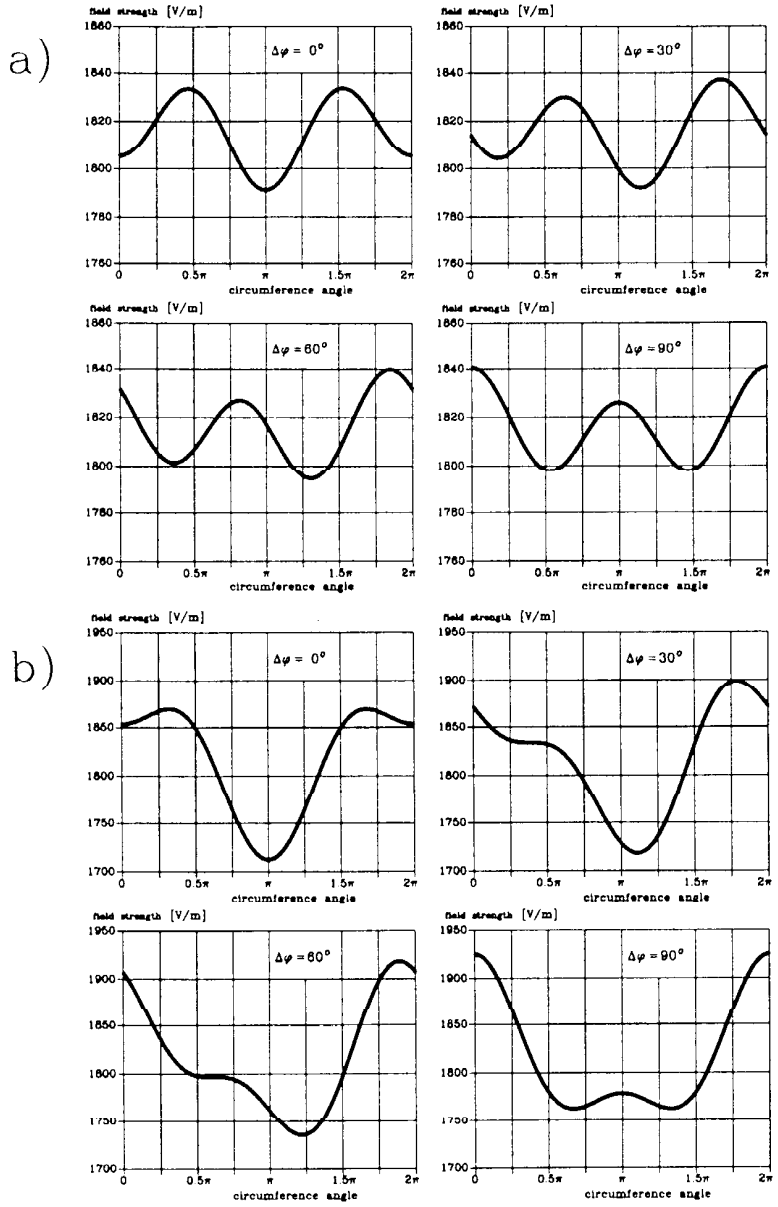

Figure 2.4: a) field strength in $50\mu m$ distance from the beam tube wall versus the circumference angle counted from the great main axis for the angle values between the great main axis and the beam shift of 0^o, 30^o, 60^o, 90^o and $\Delta l = 50\mu m$ as well as $\Delta x = 10\mu m$;
b) the same as in a), but for $\Delta l = 100\mu m$ and $\Delta x = 100\mu m$.

In figure 2.6 the angle between the scanning points is 90^o. All other numbers are the same as in figure 2.5 This gives some information about the crosstalking between two perpendicular BPM-channels for different rotational positions of the ellipticity.

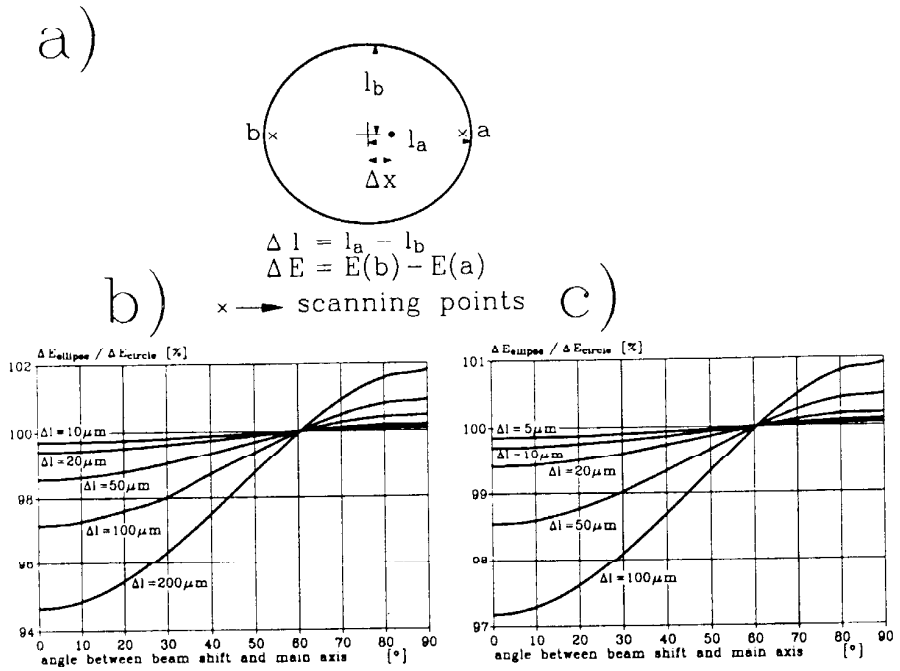

Figure 2.5: a) an eccentric beam in an elliptic beam tube;
b), c) the difference of the BPM-signals of figure 2.4 at 0^o and 180^o versus the angle between the beam shift direction and the great main axis for
b) $\Delta x = 100\mu m$ and $\Delta l = 200, 100, 50, 20, 10\mu m$ and
c) $\Delta x = 10\mu m$ and $\Delta l = 100, 50, 20, 10, 5\mu m$.

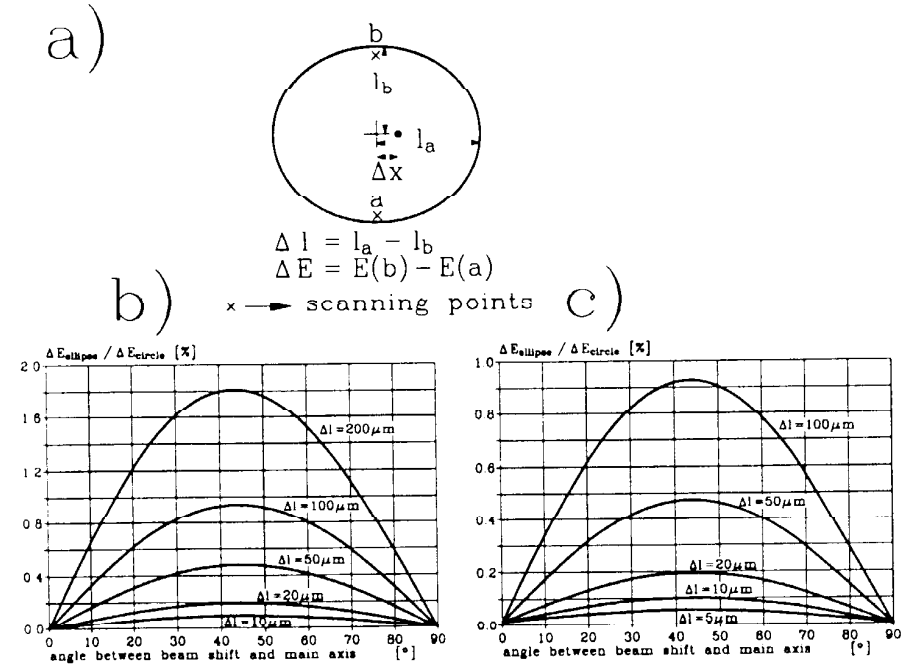

Figure 2.6: a) an eccentric beam in an elliptic beam tube;
b), c), d) the difference of the BPM-signals at 90^o and 270^o related to the beam shift versus the angle between the beam shift direction and the great main axis for
b) $\Delta x = 100\mu m$ and $\Delta l = 200, 100, 50, 20, 10\mu m$ and
c) $\Delta x = 10\mu m$. and $\Delta l = 100, 50, 20, 10, 5\mu m$.

2.3 Deviation of the Angle between the Detection Holes

In an ideal state of affairs the two detection holes of a BPM channel are separated by 180°. The second condition may be changed slightly due to mechanical deviation during drilling or etching the holes. This effect is investigated in the following plot.
In figure 2.7 the beam is shifted in the direction of the hole with an angular shift $\Delta\phi$. This shifting causes a light change of field strength.

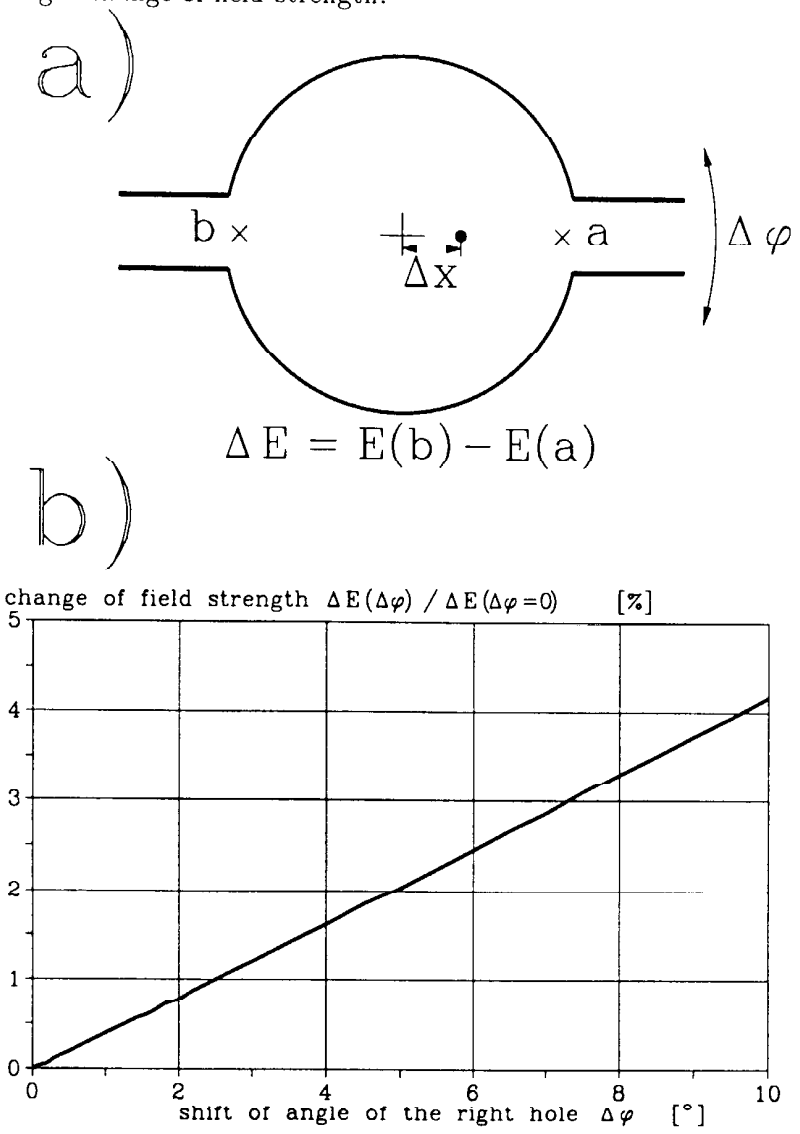

Figure 2.7: a) an eccentric beam in a round beam tube with two detection holes; b) the difference of the BPM-signals with a shift of one detection hole $\Delta\phi$ related to these for the two holes separated by exactly 180°, versus the angle variation of the right hole.

3 Deviations of the Coupling Hole

A coupling coefficient of about 2 % is assumed here. The dimensions of the configuration, which is given in appendix A and related to the projected waveguide monitor, are given in the captions. In figure 3.1 the width and length of the slot are changed in the way that the area remains constant. The width is in the same direction as the magnetic field, the length

perpendicular with that. Figure 3.2 gives some information of the sole change in width for different lengths of slots.

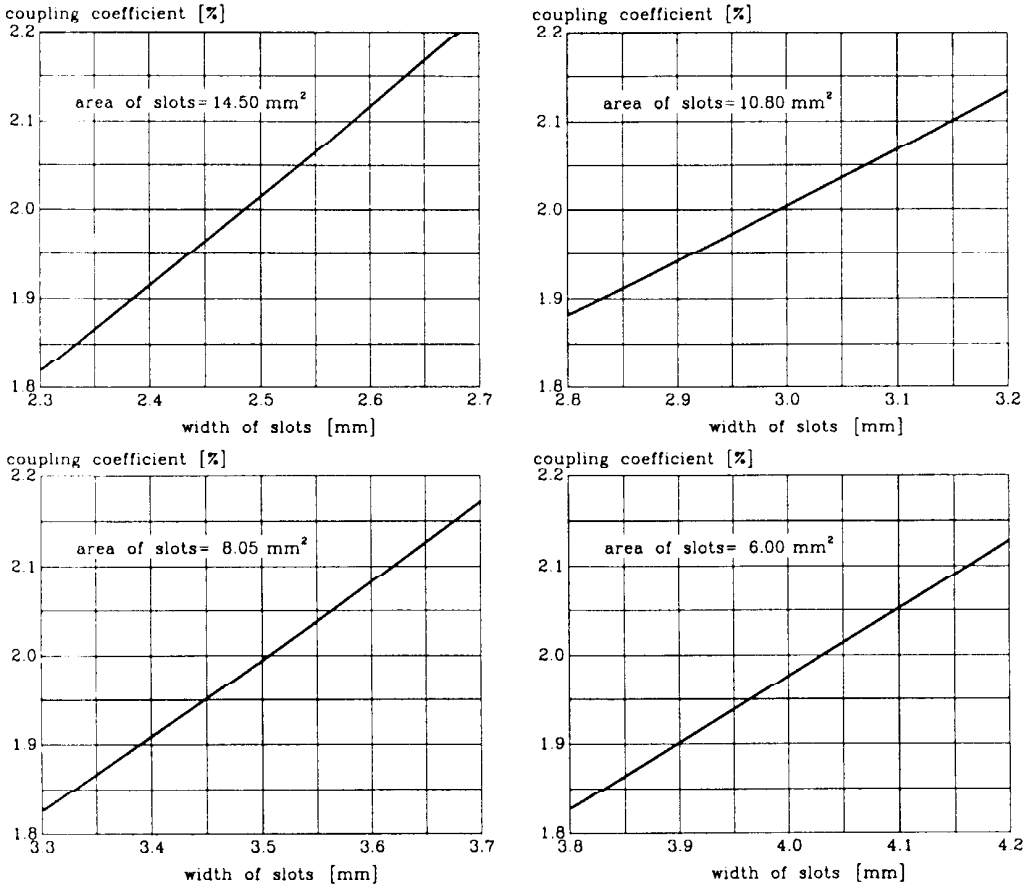

Figure 3.1: Coupling coefficient versus slot width at constant area. Dimension of TEM-line (see the appendix A) is 5x15 mm, of X-band rectangular waveguide 22.86x10.16 mm at 12 GHz.

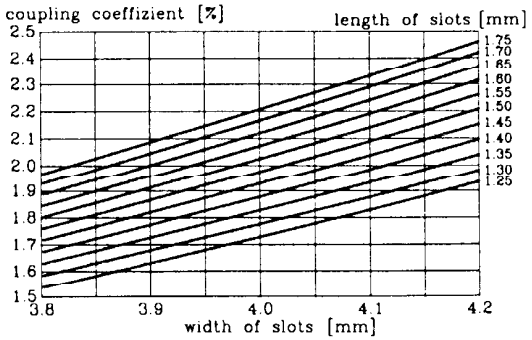

Figure 3.2: Coupling coefficient versus slot width for some slot lengths. Geometry is as in figure 4.1 at 12 GHz.

4 Conclusions - Combination of the Different Effects

4.1 Some Error Theory

If the behaviour of two deviations Y_1 and Y_2 in a physical system is strictly statistically, which means that there is no correlation, they add in the following manner called the mean square error Y_{mse}:

$$Y_{mse} = \sqrt{Y_1^2 + Y_2^2} \quad . \tag{1}$$

This could be extended to an arbitrary number of deviations.
On the other hand, if there is a strong correlation, which means 100%, then a simple addition has to be done for the entire error Y_{ma}:

$$Y_{ma} = Y_1 + Y_2 \quad . \tag{2}$$

This is also valid for an arbitrary numbers of summands.
In practice one will have something in between. For this reason a number α, let's call it correlation parameter, is defined in a way that the total deviation composed of the individual errors is given by the following formula:

$$Y_m = \left(Y_1^{2-\alpha} + Y_2^{2-\alpha}\right)^{1/(2-\alpha)} \tag{3}$$

This again is valid for an arbitrary number of errors summed up. For $\alpha = 0$ it is the uncorrelated equation (1), for $\alpha = 1$ the correlated one (2).

These cases may be representative for the errors treated in chapter 3 and 4.
In appendix B an evaluation of equation (3) is given.

4.2 Application of the Error Model

In table 4.1 some tolerable numbers of ellipticities (a), angle mismatches (b) and wall thickness deviations (c) are given for a presupposed beam position resolution. This is done for an assumed zero correlation (mean square error).

resol.	(a)	(b)	(c)	resol.	(a)	(b)	(c)	resol.	(a)	(b)	(c)
2 μm	2.4	0	0	5 μm	6.0	0	0	10 μm	12.0	0	0
	2.0	0.1	0		5.0	0.2	0		10.0	0.6	0
	2.0	0	0.003		5.0	0	0.1		10.0	0	0.015
	1.6	0.2	0		4.0	0.4	0		8.0	1.2	0
	1.6	0.1	0.003		4.0	0.2	0.1		8.0	0.6	0.015
	1.6	0	0.005		4.0	0	0.2		8.0	0	0.030
	1.2	0.3	0		3.0	0.6	0		6.0	1.8	0
	1.2	0.2	0.003		3.0	0.4	0.1		6.0	1.2	0.015
	1.2	0.1	0.005		3.0	0.2	0.2		6.0	0.6	0.030
	1.2	0	0.008		3.0	0	0.3		6.0	0.0	0.045
	0.8	0.4	0		2.0	0.8	0		4.0	2.4	0
	0.8	0.3	0.003		2.0	0.6	0.1		4.0	1.8	0.015
	0.8	0.2	0.005		2.0	0.4	0.2		4.0	1.2	0.030
	0.8	0.1	0.008		2.0	0.2	0.3		4.0	0.6	0.045
	0.8	0	0.010		2.0	0	0.4		4.0	0	0.060
	0.4	0.5	0		1.0	1.0	0		2.0	3.0	0
	0.4	0.4	0.003		1.0	0.8	0.1		2.0	2.4	0.015
	0.4	0.3	0.005		1.0	0.6	0.2		2.0	1.8	0.030
	0.4	0.2	0.008		1.0	0.4	0.3		2.0	1.2	0.045
	0.4	0.1	0.010		1.0	0.2	0.4		2.0	0.6	0.060
	0.4	0	0.013		1.0	0	0.5		2.0	0	0.075
	0	0.6	0		0	1.2	0		0	3.6	0
	0	0.5	0.003		0	1.0	0.1		0	3.0	0.015
	0	0.4	0.005		0	0.8	0.2		0	2.4	0.030
	0	0.3	0.008		0	0.6	0.3		0	1.8	0.045
	0	0.2	0.010		0	0.4	0.4		0	1.2	0.060
	0	0.1	0.013		0	0.2	0.5		0	0.6	0.075
	0	0	0.015		0	0	0.6		0	0	0.090

Table 4.1: Maximal tolerances for some required beam position resolutions concerning the following combined numbers:
(a) ellipticity (difference of semiaxes) in [μm];
(b) angle mismatch [°];
(c) wall thickness deviation for a 2.0 mm wide slot [mm].

4.3 Normalization of errors with respect to the beam displacement

The magnitude of the four above mentioned errors are given related to the signal measured for a certain beam excursion. Now assuming linearised errors the gradients are:

- displacement of the beam: $\alpha_1 = \frac{\Delta E/E}{\Delta x} = 0.079 \frac{\%}{\mu m}$,
- ellipticity: $\alpha_2 = \frac{\Delta E/E}{\Delta l} = 0.055 \frac{\%}{\mu m}$,
- wall thickness: $\alpha_3 = \frac{\Delta E/E}{\Delta d/w} = 0.32 \frac{\%mm}{\mu m}$,
  d wall thickness, w slot width,
- angle mismatch of the detectors: $\alpha_4 = \frac{\Delta E(\varphi)/\Delta E(\varphi=0)}{\Delta \varphi} = 0.42 \frac{\%}{^\circ}$,
- slotwidth with constant slotlength: $\alpha_5 = \frac{\Delta E/E}{\Delta w} = 0.057 \frac{\%}{\mu m}$
  for a slotlength of $1.5mm$.

These errors can be combined in one equation:

$$\frac{\Delta E}{E} = \alpha_1 \Delta x + \alpha_2 \Delta l + \alpha_3 \frac{d}{w} + \alpha_4 \Delta \varphi + \alpha_5 \Delta w \quad . \tag{4}$$

In the following the values equivalent to a beam displacement of $1\mu m$ are given:

- ellipticity:

$$\Delta l = 1.44 \mu m \quad , \tag{5}$$

- wall thickness:

$$\Delta(d/w) = 1.98 \quad , \tag{6}$$

- angle mismatch of the detectors:

$$\Delta \varphi = 1.88^{\circ} \quad , \tag{7}$$

- slotwidth with constant slotlength:

$$\Delta w = 1.39 \mu m \quad . \tag{8}$$

Appendix

A Bethe Theory

This tool relies on replacing small holes or slots compared to the wavelength by electric and magnetic dipols. The electric and magnetic dipole moments used here are given as follows [1]:

- Round holes
  - electric dipole moment

$$\vec{p}_e = \frac{2}{3} r^3 \varepsilon_0 \vec{E}_0 \tag{9}$$

  - magnetic dipole moment

$$\vec{p}_m = -\frac{4}{3} r^3 \mu_0 \vec{H}_0 \tag{10}$$

- Rectangular slots
  - electric dipole moment

$$\vec{p}_e = \frac{\pi}{16} d^2 l \left\{ 1 - 0.5663 \frac{d}{l} + 0.1398 \frac{d^2}{l^2} \right\} \vec{E}_0 \tag{11}$$

  - magnetic dipole moment

$$\vec{p}_m = -\frac{\pi}{16} d^2 l \left\{ 1 + 0.3577 \frac{d}{l} - 0.0356 \frac{d^2}{l^2} \right\} \vec{H}_0 \tag{12}$$

The calculation here is done for coupling between a parallel plate waveguide, which represents the beam tube containing the TEM beam excited field, and a perpendicular rectangular waveguide through a small hole or slot (figure 2.1).

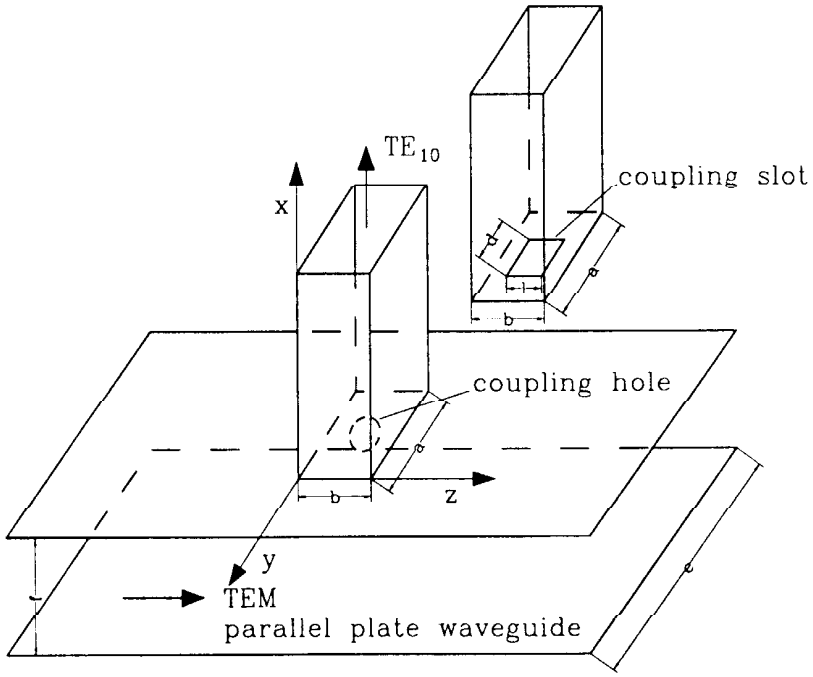

Figure 2.1: Coupling configuration between a parallel plate and a perpendicular rectangular waveguide.

To get the excitation through the slot the reciprocity theorem is applied [2]:

$$\underbrace{\oint_S \left[\vec{E} \times \vec{H}_p - \vec{E}_p \times \vec{H}\right] \cdot \mathrm{d}\vec{S}}_{\text{left side}} = \underbrace{\int V_S \Big[\underbrace{\vec{E} \cdot \vec{J}_p}_{=0} - \underbrace{\vec{E}_p \cdot \vec{J}}_{=0} + \vec{H}_p \cdot \vec{M} - \underbrace{\vec{H} \cdot \vec{M}_p}_{=0}\Big] \mathrm{d}V}_{\text{right side}} \tag{13}$$

The following quantities are used:

- excited TE_{10}-field in the rectangular waveguide: $\vec{E}$, $\vec{H}$;
- exciting electric current density: $\vec{J} = \vec{0}$;
- exciting magnetic current density: $\mathrm{j}\omega\vec{p}_m = \int \vec{M}\,\mathrm{d}V$;
- source-free test field: $\vec{J}_p = \vec{0}$, $\vec{M}_p = \vec{0}$, with $\vec{E}_p$, $\vec{H}_p$ a backward travelling TE_{10}-wave with amplitude $A^-_{10p} = 1$.

The exciting TEM-field is:

$$E_x(z) = \sqrt{Z_0}\sqrt{\frac{1}{ef}}\tilde{A}_0^+ \exp(-\mathrm{j}\beta_0 z)$$

$$H_y(z) = \frac{1}{\sqrt{Z_0}}\sqrt{\frac{1}{ef}}\tilde{A}_0^+ \exp(-\mathrm{j}\beta_0 z)$$

The excited TE_{10}-field is:

$$E_z(y,x) = \sqrt{Z_F}\sqrt{\frac{2}{ab}}\tilde{A}_{10}^+ \sin(\beta_y y)\exp(-\mathrm{j}\beta_x x)$$

$$H_y(y,x) = \pm\frac{1}{\sqrt{Z_F}}\sqrt{\frac{2}{ab}}\tilde{A}_{10}^+ \sin(\beta_y y)\exp(-\mathrm{j}\beta_x x)$$

$$H_x(y,x) = +\frac{\beta_y}{\mathrm{j}\omega\mu_0}\sqrt{\frac{2}{ab}}\sqrt{Z_F}\tilde{A}_{10}^+ \cos(\beta_y y)\exp(-\mathrm{j}\beta_x x)$$

Evaluation of the reciprocity theorem with these fields yields:

$$\begin{aligned}
\text{left side of (5)} &= -\int_{z=0}^{b}\int_{y=0}^{a}\left[\tilde{A}_{10}\frac{2}{ab}\sin^2(\beta_y y) + \tilde{A}_{10}\frac{2}{ab}\sin^2(\beta_y y)\right]\mathrm{d}y\,\mathrm{d}z \\
&= -\tilde{A}_{10}\frac{2}{ab}ab \\
&= -2\tilde{A}_{10} \\
\text{right side of (5)} &= -\mathrm{j}\omega p_m \frac{1}{Z_F}\sqrt{2}ab
\end{aligned}$$

Inserting the dipole moments results in:

- round hole

$$
\begin{aligned}
2\tilde{A}_{10} &= \mathrm{j}\omega p_m \frac{1}{Z_F}\sqrt{2}ab \\
&= -\mathrm{j}\omega\frac{4}{3}r^3\mu_0\frac{1}{Z_F}\sqrt{\frac{2}{ab}}H_{0,\mathrm{TEM}} \\
&= -\mathrm{j}\omega\frac{4}{3}r^3\mu_0\frac{1}{Z_F}\sqrt{\frac{2}{ab}}\frac{1}{\sqrt{Z_0}}\sqrt{\frac{1}{ef}}\tilde{A}_0 \\
&\Rightarrow \\
\left|\frac{\tilde{A}_{10}}{\tilde{A}_0}\right| &= \omega\frac{2}{3}r^3\frac{\mu_0}{\sqrt{Z_F Z_0}}\sqrt{\frac{2}{abef}} \qquad (14)
\end{aligned}
$$

- rectangular slot

$$
\begin{aligned}
2\tilde{A}_{10} &= \mathrm{j}\omega p_m \frac{1}{\sqrt{Z_F}}\sqrt{\frac{2}{ab}} \\
&= -\mathrm{j}\omega\frac{\pi}{16}d^2 l\left(1+0.3577\frac{d}{l}-0.0356\frac{d^2}{l^2}\right)\mu_0\frac{1}{\sqrt{Z_F}}\sqrt{\frac{2}{ab}}\frac{1}{\sqrt{Z_0}}\sqrt{\frac{1}{cf}}\tilde{A}_0 \\
&\Rightarrow \\
\left|\frac{\tilde{A}_{10}}{\tilde{A}_0}\right| &= \omega\frac{\pi}{32}d^2 l\left(1+0.3577\frac{d}{l}-0.0356\frac{d^2}{l^2}\right)\frac{\mu_0}{\sqrt{Z_F Z_0}}\sqrt{\frac{2}{abef}} \qquad (15)
\end{aligned}
$$

B Application of the Error Model

In figure B.1 equation (3) is applied for some added errors expressed in percents. To find out the right value for α is a matter of mechanical and experimental work.

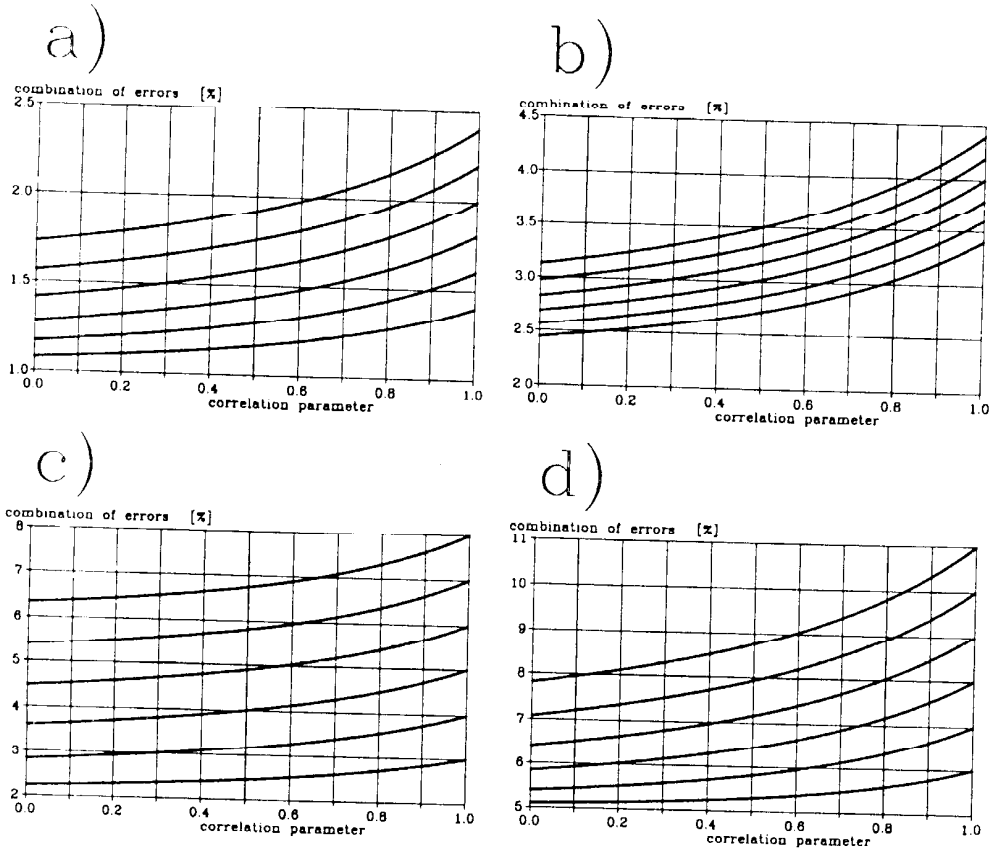

Figure B.1: Composition of two errors versus the correlation parameter α;
a) 5% combined with $1, 2, 3, 4, 5, 6\%$,
b) 2% combined with $1, 2, 3, 4, 5, 6\%$,
c) 2% combined with $1.4, 1.6, 1.8, 2.0, 2.2, 2.4\%$,
d) 1% combined with $0.4, 0.6, 0.8, 1.0, 1.2, 1.4\%$.

References

[1] S. Kurennoy, *Pumping Slots: Coupling Impedance Calculations and Estimates*, SSCL-636, August 1993

[2] H. Henke, *Bethe's Theory of Diffraction by Small Holes*, TET-NOTE 96/04, TU-Berlin, internal note